# Development of CMIP6-based climate scenarios for Japan using statistical method and their applicability to impact studies

**Noriko N. Ishizaki[1], Hideo Shiogama[1], Naota Hanasaki[1] and Kiyoshi Takahashi[1]**

[1] National Institute for Environmental Studies, Tsukuba, Japan

Corresponding author: Noriko N. Ishizaki (ishizaki.noriko@nies.go.jp)

**Key Points:**

- We developed a statistically downscaled climate scenarios in Japan based on five general circulation models selected from the Coupled Model Intercomparison Project Phase 6 to facilitate impact assessments.
- Similar increasing trend was found for the temperature and precipitation between CMIP5- and CMIP6-based climate scenarios, while CMIP6-based scenario showed a smaller biases for the underlying GCM. Addition of the moderate emission scenario for CMIP6-based scenario enable us to consider wider range of the possible future.
- Several threshold-based indices derived from the climate scenarios was evaluated. They agreed with the observed values for the historical period. For the future, we can discuss the possible future change of indices in comparison with the historical values. Development of the bias-corrected climate scenarios has enabled the broader impact assessment community in Japan to study various climate impacts on a CMIP6 basis.

## Abstract

Climate scenario dataset are indispensable for assessing future climate impacts. In this study, we developed statistically downscaled climate scenarios in Japan using modified bias correction method based on five general circulation models selected from the Coupled Model Intercomparison Project (CMIP) Phase 6 to facilitate impact assessments and adaptation strategies. Modification of time window of the original correction method results in successful agreement with the observed seasonal change of variables in each grid. The original CMIP6 models have a relatively small bias compared to CMIP5 models. The CMIP6-based bias-corrected scenarios are available for use with the emissions scenario of representative concentration pathway (RCP) 4.5 in addition to RCP2.6 and RCP8.5. Several temperature-related indices derived from the CMIP6-based climate scenarios agreed well with observations. The number of extremely hot days and nights increased nonlinearly in the future with additional global warming. An increase in the global warming level from 1°C to 2°C above the early 1900s would increase the probability of the number of extremely hot days per year exceeding the 2018 case by 4.1 times. The development of bias-corrected climate scenarios facilitates the study of various climate impacts on a CMIP6 basis.


## 1 Introduction

Future climate projections are generally obtained from global circulation models (GCMs) and then used to assess the impacts of a changing climate. However, GCM simulations often show systematic bias. If the impact linearly depends on the climate input data, we can use the anomaly with respect to a reference period, but this is not possible in many cases. Bias must be treated carefully in the context of climate impact simulations (e.g., Ishizaki et al. 2020; Hempel et al. 2013; Gomez-Garcia et al. 2019; Iizumi et al. 2017; Maraun et al. 2017).

Bias correction (BC) is essential if the impacts are activated when certain absolute climatic thresholds are exceeded. One typical example is the heat index, which is closely related to human mortality. Extreme heat and frost are often evaluated using the definition of the daily maximum or minimum temperature. To manage acute health risks, it is important to know how the number of extreme hot and cold days will change in each region using bias-corrected data. Several studies have demonstrated that BC can provide not only a substantial improvement of the absolute present climate status, but also a more robust climate change signal for threshold-based indices (e.g., Dosio 2016, Iturbide et al. 2022).

Long-term data are essential for climate impact assessments in some sectors. For example, several studies have demonstrated the effect of acclimatization associated with heat-related mortality (e.g., Fujibe et al. 2018; Kodera et al. 2019; Ng et al. 2014). Ng et al. (2016) showed that mortality increases for a 1°C temperature increase have become smaller over time. This suggests that not only the average temperature at a certain time in the future, but the temperature record up to that time will be important when assessing the heat risk considering the acclimatization effect. Therefore, the use of a long-term time series is more suitable than time slice experiments for climate projections to study future heat risk. Developing long-term scenarios by dynamical downscaling is difficult due to the computational cost, and most high-resolution climate simulations based on dynamic downscaling across Japan have been derived by 20-year time slice experiments (e.g., Murata et al. 2017, Sasaki et al. 2011). On the other hand, statistical downscaling and BC can be inexpensively implemented to create long-term regional

climate projections. In this way, the combination of statistical downscaling and BC plays an important role in applying climate scenarios to impact assessments of climate change.

Bias-corrected projections are available for the multiple GCMs used in Coupled Model Intercomparison Project (CMIP) Phase 5 as a long-term climate scenario in Japan (Ishizaki et al. 2020, Nishimori et al. 2019). The climate scenarios developed by Ishizaki et al. (2020) are 1 km meshed daily data using the four CMIP5 GCMs, which were bias-corrected based on the BC method proposed by Iizumi et al. (2010). Biases were generally eliminated, but the seasonal change in the monthly averaged corrected data tended to follow that of the parent model (Ishizaki et al. 2020). However, CMIP6 data are now already available and Intergovernmental Panel on Climate Change (IPCC) assessment reports are based on CMIP6 outputs (IPCC, 2021), although bias-corrected data applied to CMIP6 are not currently available. It is therefore of interest to determine how the climate scenarios differ between CMIP5 and CMIP6. We also investigated how the results could be improved by modifying the BC methods employed in Ishizaki et al. (2020).

In this study, we developed a bias-corrected climate scenario based on the multiple GCMs of CMIP6. We assessed whether CMIP6-based climate scenarios can be treated as equivalent to CMIP5-based climate scenarios, and if not which aspects differ. As an example of the application of a climate scenario, we evaluated the heat mortality-related indices in Japan. Although we did not assess human mortality directly, we examined whether the relevant indicators were consistent with those observed in past periods and further considered the sensitivity of future changes. Furthermore, we reconsidered the dependence of the indices on the global warming levels (GWLs) using bias-corrected scenarios. Based on the results of the analysis, we discuss the applicability of climate scenarios for various impact assessments.

## 2 Data and Method

We developed statistical downscaled climate scenarios based on CMIP6. To promote the intercomparison of climate change impact assessments considering the limited number of scenarios that could be handled, we selected a few GCMs from a large model ensemble. Based on a method that objectively constructed a subset that covered a wide range of uncertainty in the CMIP6 ensemble (Shiogama et al. 2021), five GCMs were selected: MRI-ESM2.0, MIROC6, ACCESS-CM2, IPSL-CM6A-LR, and MPI-ESM1–2-HR. The basis for model selection was different from that used in the CMIP5-based climate scenarios in Japan (Hanasaki et al. 2012; Ishizaki et al. 2020). Instead of the representative concentration pathway (RCP) for CMIP5, emissions scenarios for CMIP6 were represented using a combination of shared socioeconomic pathways (SSPs) and RCPs. We selected SSP1-RCP2.6 (SSP126) and SSP5-RCP8.5 (SSP585) to facilitate a comparison with CMIP5-based climate scenarios, while SSP2-RCP4.5 (SSP245) was additionally selected as an intermediate emissions scenario. Agro-Meteorological Grid Square Data (AMGSD; Ohno et al. 2016) were used as reference data for the historical period.

Daily data derived from GCMs were interpolated to a 1 km mesh using bilinear interpolation and then bias-corrected. The BC was based on the cumulative distribution function-based downscaling method (CDFDM) proposed by Iizumi et al. (2010; 2011; 2012; 2014; 2017). This is a non-parametric method, in which the bias is identified and corrected in each percentile. Once GCM error was defined by comparison with the reference data in the calibration period, the error was removed from the empirical cumulative distribution functions (CDFs) for each BC period with the assumption that the error-percentile relationship does not change over time. The

relationship was specified over a half-year period in the original method. We refer to the original method as CDFDM-O in this paper.

The BC was applied to eight variables: the daily maximum, minimum and mean temperature, precipitation, global solar radiation, surface wind speed, surface relative humidity, and downward longwave radiation. The calibration period was set from 1980 to 2018. The GCM data for this period consisted of the historical experiment for 1980–2014 and the SSP585 experiment for 2015–2018. The calibration period for the surface wind speed, relative humidity, and downward longwave radiation was from 2008 to 2018 due to the availability of the reference data. We used a 39-year moving window (11-year for the variables with a short calibration period) to match the length of the BC period and the model calibration period. Specifically, BC was conducted for the historical period (1900–1938, 1939–1977, 1976–2014) and future period (2015–2053, 2054–2092, 2062–2100). Bias correction data were created twice for 1976–1977 and 2062–2092 because the BC periods overlapped. For the overlapping period, we only used the BC data derived from the latter BC period. The time window was set to a half-year period in the CDFDM-O (Iizumi et al. 2010), but was modified to monthly in this study so that the monthly value corresponded to that of the observation in the calibration period. For the temperature (daily maximum, minimum, and mean) and downward longwave radiation, the linear trend of the BC period was preserved. We referred to the modified method as CDFDM-M. The BC method modified the statistical properties of climate simulations to match the observations for each region, so that changes in the indices, as defined by the frequency of exceeding a threshold, could be properly evaluated. Of the eight bias-corrected variables, daily maximum and minimum temperatures up to 2100 were selected for analysis.

Various climate indices can be created from BC data, but we calculated and examined a heat-related index as a specific example, i.e., the annual number of days when the daily maximum temperature exceeded 35°C (TX35), the annual number of days when the daily minimum temperature exceeded 25°C (TN25), and the annual number of days when the daily minimum temperature was below 0°C (TN0). The annual maximum consecutive days for days meeting each threshold was also evaluated (CTX35, CTN25, and CTN0, respectively). We examined their dependency on the emissions scenarios and GCMs. The locations of the automated meteorological data acquisition system (AMeDAS; total 743 sites) were used to calculate the index values per site in Japan.

## 3 Differences in the climate scenarios based on CMIP5 and CMIP6

First, we describe the differences in the climate scenarios between CMIP5 and CMIP6. Figure 1 shows the 20-year running mean of temperature and precipitation over Japan. Selected original CMIP6 GCM outputs had an apparently warm bias over Japan compared to AMGSD (Fig. 1a). The CMIP5 GCMs had larger biases, although they captured the recent warming trend. One common reason for the overestimation was the difference in altitude of the grids in the GCMs. A coarse grid model cannot represent high mountains and the temperature tended to be overestimated without the elevation correction. The warm bias was generally removed by applying CDFDM-M (Fig. 1c,d). The ensemble mean for surface temperature was 12.0°C for RCP2.6 (SSP126) and 12.3°C for RCP8.5 (SSP585) around 2040 for both CMIP5- and CMIP6-based climate scenarios. Regarding the GCM uncertainty, CMIP6-based scenarios were different from CMIP5-based scenarios in that the range between RCP8.5 and RCP2.6 overlapped considerably in the 2040s and they had a narrower range. Although the number of GCMs was

different, the impact of the different emissions scenarios on climate change over the next few decades would be relatively small. In the second half of the 21st century, the difference between RCP2.6 and RCP8.5 became more pronounced for both datasets. The addition of RCP4.5 enabled us to cover a wide range of possible futures.

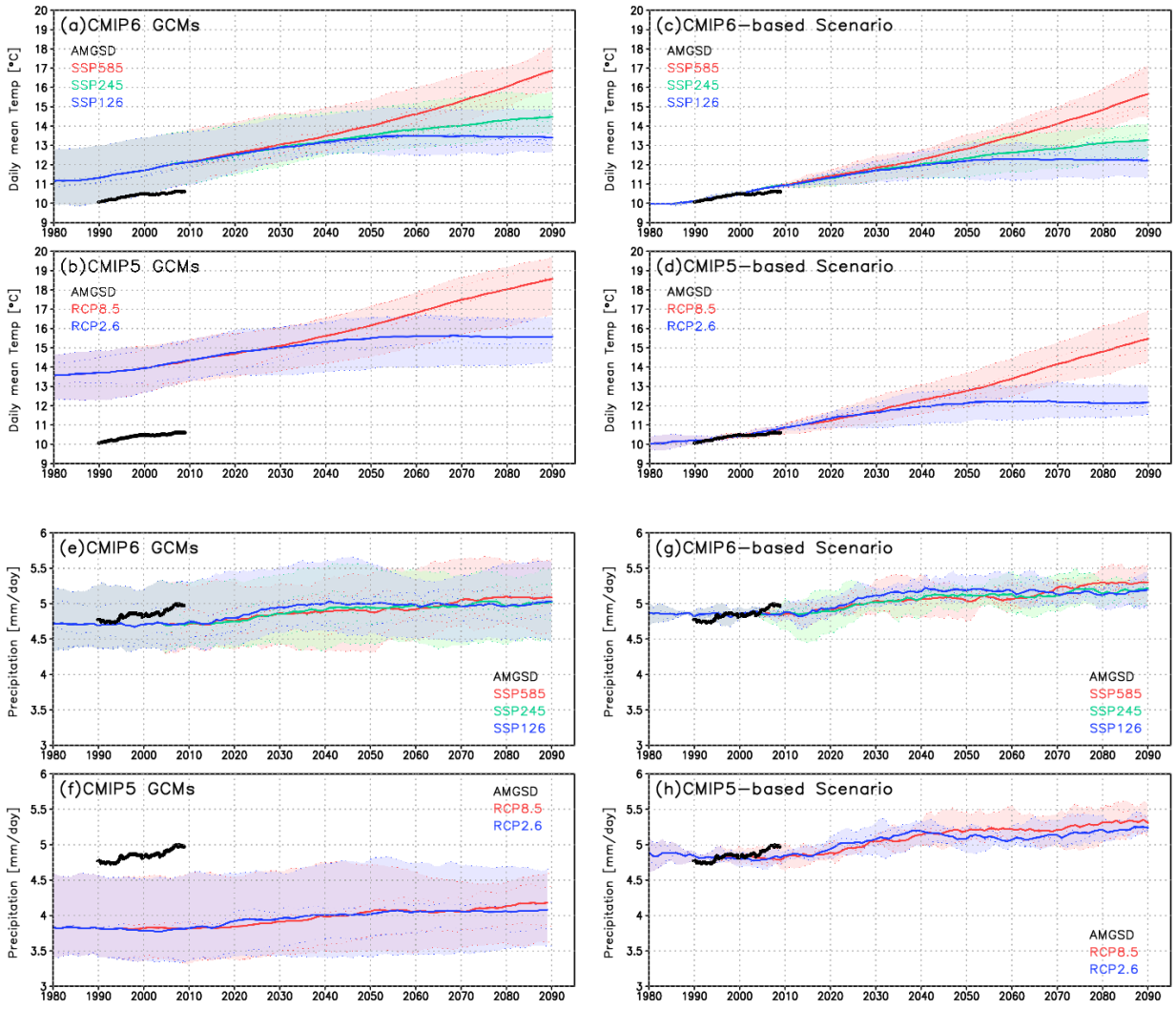


**Figure 1. Twenty-year running mean time series of the daily mean temperature (a-d) and precipitation (e-h) averaged across Japan based on (a, e) selected original CMIP6 GCMs, (b, f) selected original CMIP5 GCMs, (c, g) CMIP6-based scenarios and (d, h) CMIP5-based scenarios. Solid lines indicate the ensemble mean of bias-corrected data based on selected GCMs in each emissions scenario and shade indicated the maximum and minimum among selected GCMs. The thick black line denotes the reference data AMGSD.**

All of the GCMs selected from CMIP5 significantly underestimated the precipitation (Fig. 1f). For CMIP6, some GCMs overestimated and others underestimated the precipitation, resulting in the ensemble mean providing a reasonable representation. Bias-corrected precipitation tended to increase through the mid-21st century under both RCP2.6 and RCP8.5 (Fig. 1g,h). The ensemble mean under the RCP2.6 scenario was higher than under RCP8.5 until the mid-21st century, while precipitation at the end of the 21st century was higher under RCP8.5 for both datasets, increasing by up to 10% compared to 2000. According to the IPCC, Japan is located at a boundary between regions that will become drier and wetter with additional global warming, while it is very likely that heavy precipitation will intensify and become more frequent in most regions (IPCC 2021). This indicates a large uncertainty in the future changes in average precipitation.

Comparison of climate scenarios based on CMIP5 and CMIP6 implied that the general features of the temperature and precipitation over Japan were similar. The biases of the original GCMs selected from CMIP5 were generally larger than those from CMIP6. The CMIP6-based climate scenarios were also available for the moderate emissions scenarios, enabling their impacts to be assessed in various possible future changes, which was not possible in the CMIP5-based climate scenarios.

## 4 Evaluation of the modified BC method

To confirm that the BC was working correctly, Fig. 2 shows the bias-corrected monthly temperature and precipitation based on MIROC6 at six locations for the 25-year average from 1991 to 2015. The white bars show seasonal variation in temperatures derived from the original MIROC6 data that was similar to, but generally lower than, the observations shown in the black bars. Temperatures corrected by CDFDM-M were reproduced as well as those corrected by CDFDM-O. The root mean square errors (RMSEs) of the mean temperature in the summer (June to August) were 2.47°C, 0.16°C, and 0.08°C for the MIROC6 output, and the CDFDM-O and CDFDM-M corrections, respectively. The corresponding values in the winter (December to February) were 4.82°C, 0.12°C, and 0.22°C, respectively. Both correction methods successfully reduced the inherent bias in the GCM.

The GCM precipitation data displayed different seasonal changes from the observations in many locations. For example, the precipitation in June was too high in Tokyo, Osaka, and Naha. For the CDFDM-O correction, the seasonal changes were similar to those in the GCM. This was reflected in the RMSE. For JJA, the RMSEs were 2.19, 1.37, and 0.32 mm day-1 for the GCM, CDFDM-O, and CDFDM-M, respectively. For DJF, the values were 1.71, 1.15, and 0.13 mm day-1, respectively. The results showed that the corrected precipitation using the CDFDM-M was in good agreement with the observations in the current climate, which was achieved by the modification of the time windows of CDFDM-O.

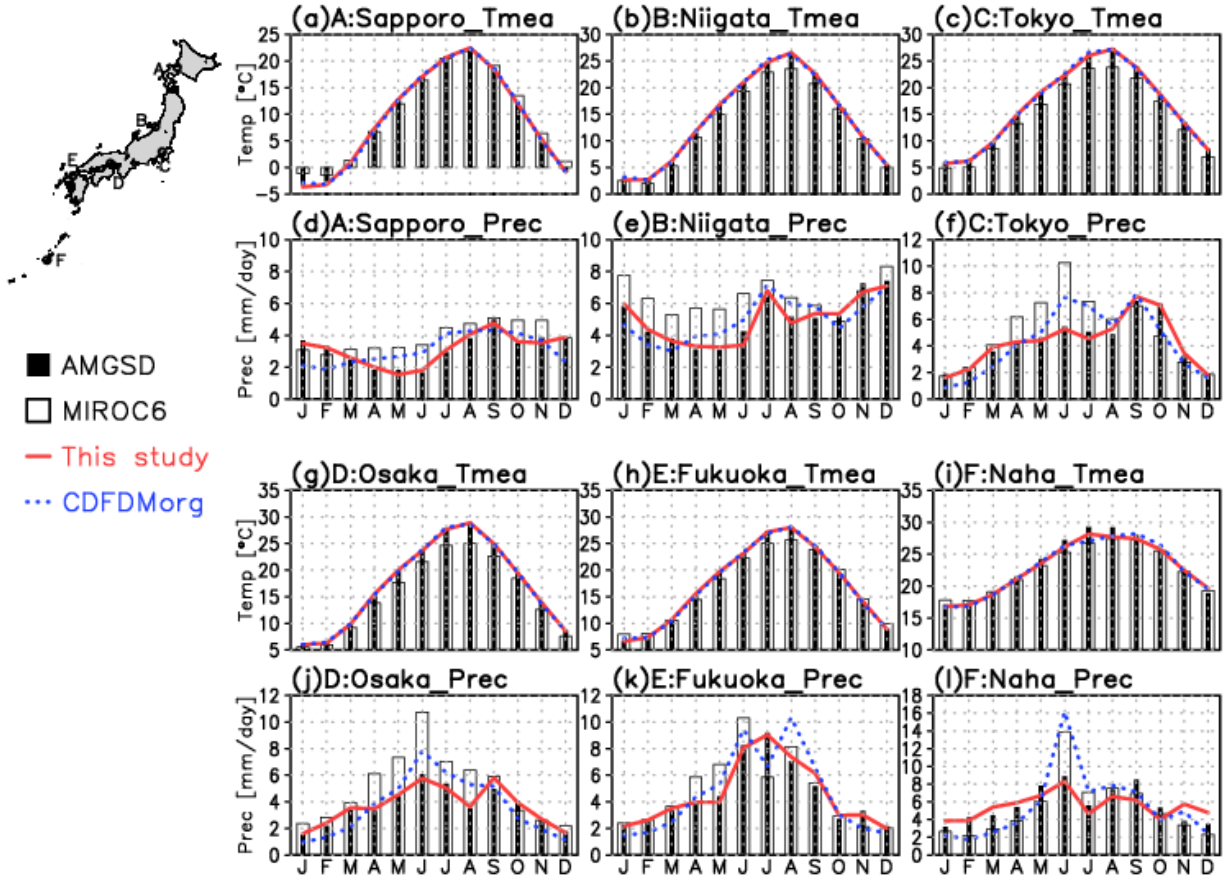


**Figure 2. Monthly variation in the climatological mean of the daily mean temperature (a-c, g-i) and precipitation (d-f, j-l) at six stations shown in the left panel. Black and white bars indicate the AMGSD and interpolated MIROC6 data. Red solid and blue dashed lines show the bias-corrected values using the CDFDM-M and CDFDM-O, respectively.**

## 5 Application to heat-related indices

### 5.1 Evaluation of heat-related indices derived from bias corrected climate scenarios

To evaluate the validity of the bias-corrected climate scenarios, we examined the reproducibility of temperature-related indices. Figure 3 shows the TX35 values for the historical climate and their future changes. The future changes showed the ensemble mean of the five GCMs. In most areas, except for high-altitude regions, we observed a day with the daily maximum temperature exceeding 35°C during 1901–1950. A large TX35 value was observed in the western part of the Kanto Plain, in the vicinity of Nagoya and Osaka, the western Kyushu region, and the coastal area of Niigata Prefecture, which are areas where the föehn phenomenon often occurs. In the 2040s, the average TX35 value was projected to increase. An increasing range was prominent in areas where the historical occurrence was high. There were no clear differences among emissions scenarios in the 2040s. The total area where the TX35 threshold

was exceeded every year on average was expected to be 2.1 to 3.8 times larger than the historical level. In the 2060s, there were clear differences among emissions scenarios. There was little difference in the SSP126 scenario from the 2040s, while the SSP585 scenario was expected to have about twice as many hot days as the 2040s. It was projected that the climatological occurrence of the TX35 would increase by 5 days in most lowland areas in eastern and western Japan under the SSP245, larger than the increase for SSP126.

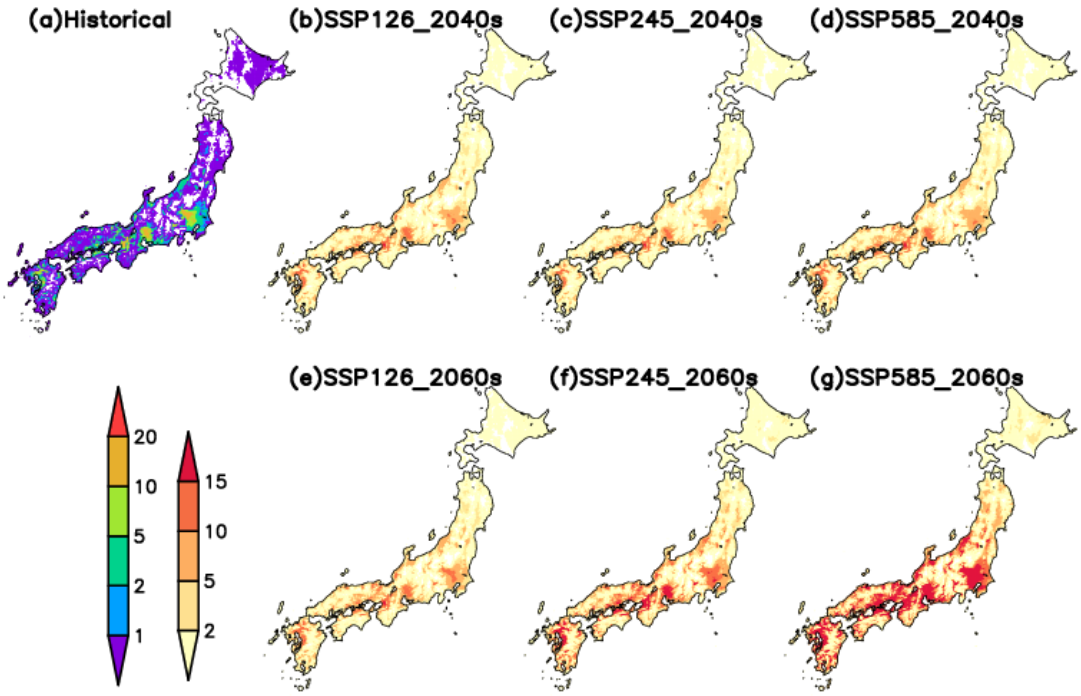


**Figure 3. Ensemble mean of the annual number of the TX35 for (a) present climate (2001–2020) and (b-g) future change: (b) 2040s (2031–2050) in SSP126, (c) 2040s in SSP245, (d) 2040s in SSP585, (e) 2060s (2051–2070) in SSP126, (f) 2060s in SSP245, and (g) 2060s in SSP585. The colour bar on left (right) side is for present climate (future change).**

To examine model variability, the variation in the TX35 and CTX35 indices over time in Tokyo is shown in Fig. 4. The representation of historical TX35 values based on the bias-corrected data is in good agreement with the observed values. In the future, although there was variability among the GCMs, SSP126 showed a small change in the number of extremely hot days after 2050, SSP245 showed a gradual increase toward the end of the 21st century, and SSP585 showed a large increasing trend. This was accompanied by an increase in the maximum number of consecutive extremely hot days. In the historical period, the CTX35 value was less than three, but this increased to 4–8 days in SSP126, 6–12 days in SSP245, and 10–26 days in SSP585 at the end of the 21st century. Fujibe et al. (2018) found that daily heatstroke mortality was higher for cases with a high temperature on the preceding few days (up to a week) due to accumulated heat stress. Their findings implied further increased health risk with global warming. At the same time, we found that the first date in the year when the TX35 threshold was exceeded tended to occur earlier and the last date tended to occur later (figure not shown). The TN25 index was also projected to increase with global warming as expected (Figure S1 in

supporting information), with a high value in coastal areas. On the other hand, TN0 was projected to decrease substantially (Figure S2 in supporting information). The temporal changes in TN0 and CTN0 revealed that BC worked well for the historical period (Figure S3 in supporting information).

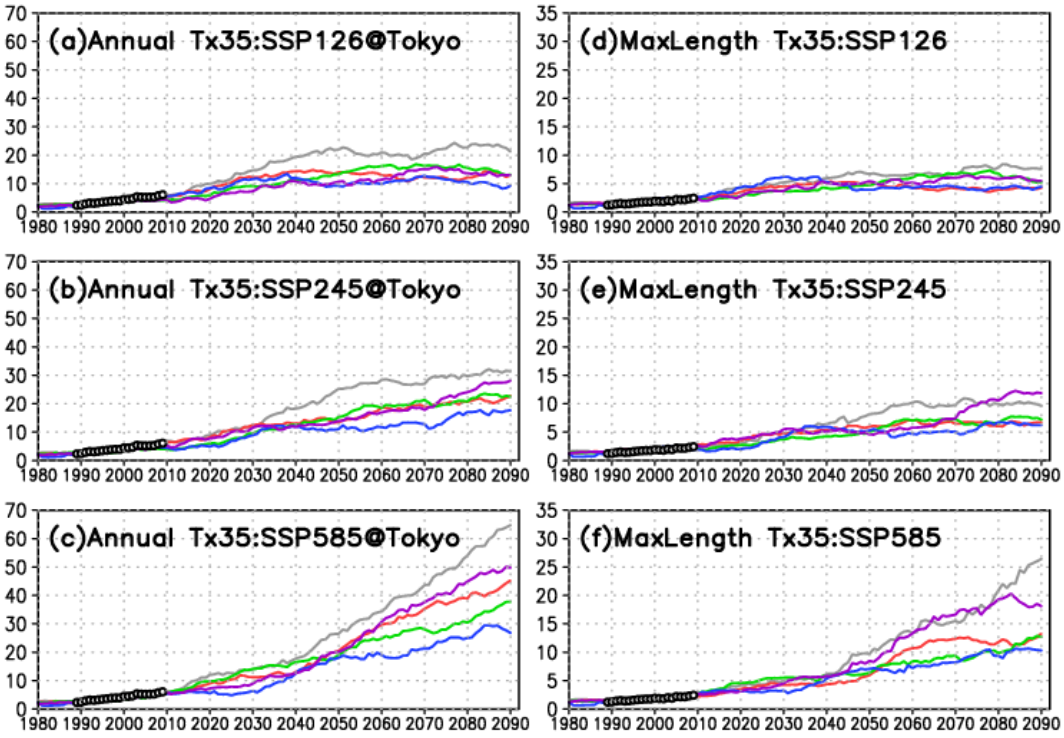


**Figure 4. Twenty-year running mean of the annual number of TX35 in Tokyo with (a) SSP126, (b) SSP245, and (c) SSP585. The maximum number of consecutive days of TX35 with (d) SSP126, (e) SSP245, and (f) SSP585. The five coloured lines indicate each GCM and solid lines with white circles show the observed value.**

### 5.2 Dependences of the indices on the GWL

We investigated the dependencies of the indices derived from the bias-corrected scenarios on the GWL. The mean TX35 per total number of station points in Japan (MTX35) is plotted in Fig. 5. The nearest grids to the 743 AMeDAS stations were used. The GWLs were defined by the increase in temperature from the average of 1901–1950. The GWL from 2010 to 2018 ranged from 0.6 to 1.0. Observations made in recent years were also plotted. The nonlinear increase in MTX35 with GWL is generally consistent with Imada et al. (2019), although the number of observations used in the two studies was different. The TX35 per site observed in Japan tended to increase with GWL, but the larger the global temperature increase, the larger the uncertainty. The increase in MTX35 was not pronounced during the period with a small temperature increase; however, if the GWL exceeded 2°C the TX35 per site would be much higher than the present level. As shown in Fig. 5b, the probability of exceeding MTX35 for 2018, when various incidents of heat-related damage occurred, was generally 9.7% under a GWL of 1°C. However, the probabilities increased

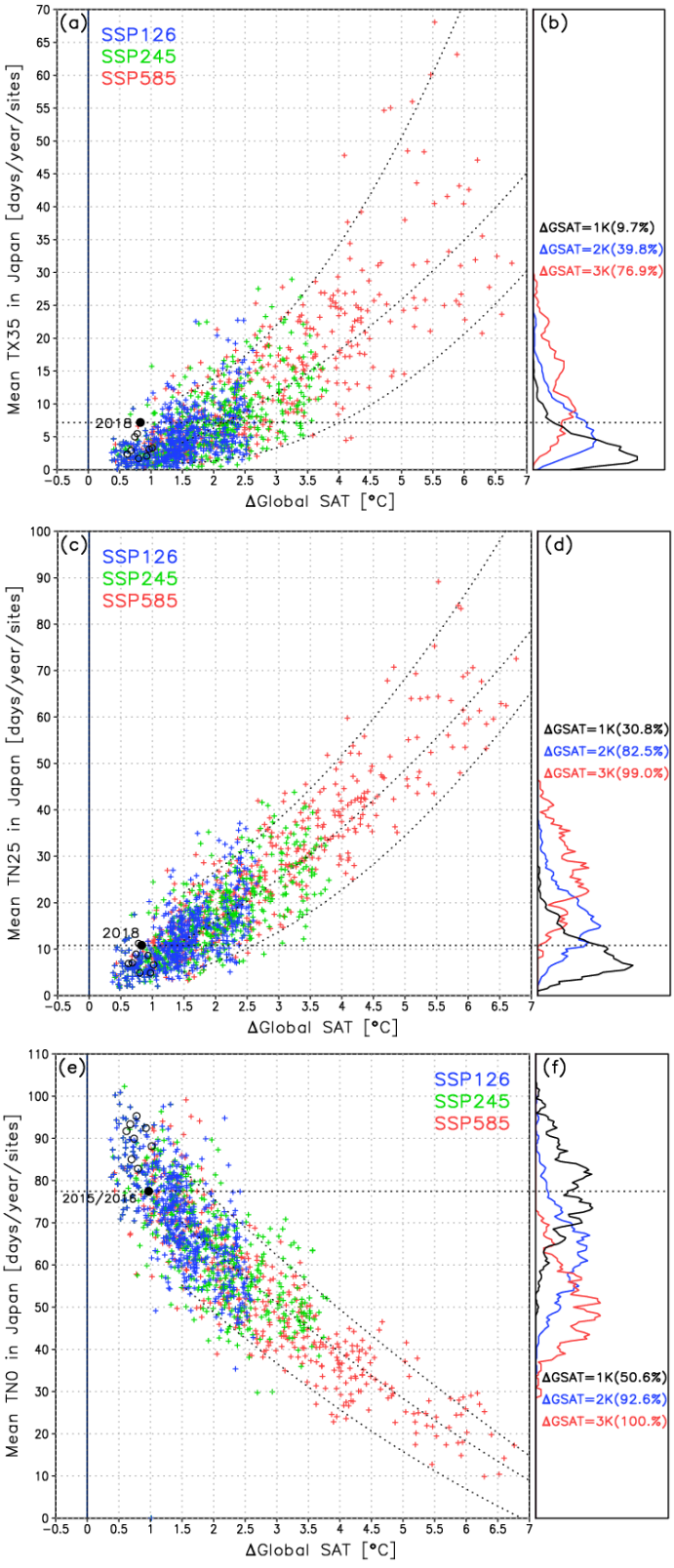


**Figure 5. Mean value of (a) TX35, (c) TN25, and (e) TN0 per site per year from 2000 to 2100 relative to the global mean temperature increase (MTX35, MTN25, and MTN0, respectively).**

**The GWL was defined by the deviation from the 1901–1950 average. It was calculated from the nearest grid corresponding to 743 AMeDAS stations. The figures on the right side (b, d, f) show the probability density distribution when the GWL was 1, 2, and 3 K. The white circles in (a) and (c) indicate the observed values from 2010 to 2018, and those in (e) show the observed MTN0 for the winter season of 2010/2011 to 2017/2018. Black dots indicate the severest events in recent years; 2018 for MTX35 and MTN25 and 2015/2016 for MTN0. The blue, green, and red marks show SSP126, SSP245, and SSP585, respectively. The dashed lines are fitting curves derived from the 5, 50, and 95 percentile MTX35 in each bin of the GWLs. The figures on the right side (b, d, f) show the probability density distribution when the global warming level was 1, 2, and 3 K. Each number in parentheses in (b) and (d) represents the probability of exceeding the largest event depicted by the black dots in each left panel. For (f), the number indicates the probability of falling below the smallest event.**

to 39.8% and 76.9% when the GWL reached 2°C and 3°C, respectively. Therefore, the probability of exceeding the maximum historical MTX was more than four times greater for a GWL of 2°C than for 1°C. When we estimated the 50 percentile value of MTX35 in each bin, MTX35 increased from 2.3 to 6.3 when GWL changed from 1°C to 2°C. The MTX35 at a GWL of 1°C was similar to the results of Imada et al. (2019) if we considered the differences with the reference period to define the GWL. However, our estimation of MTX35 at a GWL of 2°C seemed to be larger than that reported by Imada et al. (2019). It should be noted that a greater MTX35 may occur when multiple GCM results are used. This shows the importance of accumulating global warming countermeasures for several decades from now to minimise the global warming impacts on health and other sectors. Factors contributing to the increase in MTX35 per site included the increase in TX35 at sites where it had not been observed before and an increase in the frequency of TX35 at sites where it had been observed before. For the former, the TX35 increased depending on the diurnal range in each region. For the latter, we found that the earlier occurrence of TX35 before mid-summer contributed more to the annual occurrence (figure not shown).

The mean TN25 in Japan (MTN25), calculated using the daily minimum temperature at the AMeDAS stations, displayed an increasing trend even under a low GWL (Fig. 5c), with less variability than in MTX35. The MTN25 increased by about 10 days per 1°C warming, but the increase was larger with a high GWL. The MTN25 for 2018 was the second highest during 1980–2018. The probability of exceeding MTN25 in 2018 was 30.8%, 82.5%, and 99.0%, under GWLs of 1°C, 2°C, and 3°C, respectively. It is necessary to consider countermeasures against heat stroke risks caused by high temperatures at night as well as daily maximum temperatures.

The decrease in mean TN0 in Japan (MTN0) during winter was also closely associated with mortality (Fig. 5e). The MTN0 in Japan, which was 80–95 in recent years, will decrease substantially in response to global warming. Among the three indices, the change in TN0 was very sensitive to the GWL. When the GWL was 2°C, the decrease per 1°C global warming was approximately 30 days. When the GWL exceeded 2°C, the decrease became smaller, but the MTN0 was expected to be about half of the present level at that time. During the 2015/2016 winter season, the annual occurrence was the second smallest for the period from 1980/1981 to 2017/2018. At that time, many areas in Japan implemented measures such as water withdrawal restrictions because there was a risk for serious drought during the summer season (MLIT, 2016). The probability that MTN0 would be smaller than the value in 2015/2016 was 49.1%

even under a GWL of 1°C. The probability increased to 91.8% and 100% when the warming level was 2°C and 3°C, respectively.

## 6 Discussions

It is important to note that the climate scenarios developed in this study were based on statistical data, and dynamic effects were not directly taken into account. Therefore, the climate scenarios do not directly depict meteorological events. For example, the föehn phenomenon, which is caused by the mechanical effect of high mountains and generates warm and dry winds on the leeside of the mountains, causes hot days. The BC used in this study was based on the past frequency of such phenomena at each location and did not take into account changes in the frequency of föehn occurrence due to the changes in the circulation field in each GCM. However, unless the climatological circulation patterns change significantly, it is inconceivable that föehn conditions will occur frequently in areas where they have not been observed in the past. Thus, we believe that the regional differences were generally well represented. The precipitation should be treated with caution because it cannot represent the typical spatial extent of precipitation system in each season and region.

For the heat mortality-related indices, all three indicators derived from the bias-corrected data agreed with observations. However, there were greater uncertainties in the future projections for a given GWL compared to previous studies based on a single GCM. One example of this was the comparison of the future changes in the indices reported by Japan's Climate Change 2020 (JMA and MEXT, 2020), in which the TX35, TN25, and TN0 were also described in the context of the change between future and present stages under the RCP2.6 and RCP8.5 scenarios. Our results do not conflict with those of that report, but they have a larger range of uncertainty. For example, the report showed that the mean TX35 in Japan would increase by 19.1 days, with a standard deviation of 5.2 days, at the end of the 21st century under the RCP8.5 scenario, while our results ranged from 14.4 to 40.5 days depending on the GCM.

Another example is the change in MTX35 with GWL. The nonlinear increase in MTX35 with GWL is generally consistent with previous studies (Imada et al. 2019; Fischer and Knutti 2015). The estimated change in the 50 percentile value of MTX35 at GWLs of 1°C and 2°C was higher than that reported by Imada et al. (2019) due to the larger uncertainty. Although there were more than 500 samples per bin at GWLs below 2°C, the number of samples was relatively small. However, these results imply that the uncertainty due to GCMs was still present in the future projections and we should therefore take into account the uncertainty stemming from the use of different GCMs. Climate projections with an uncertainty range sometimes tend to be avoided by data users, but it is recommended to use climate projections from multiple GCMs as long as the plausibility is unknown.

The climate scenarios developed in this study are in good agreement with observations for the historical period of 1991 to 2015, even on a monthly basis, and thus are useful for properly assessing the impact of climate change. The scenarios based on the CMIP6 models, which had a relatively small bias, were also applied to intermediate emissions scenarios. The climate scenarios were developed at a high horizontal resolution of a 1 km mesh, which allowed for region-specific impact assessments in combination with socioeconomic scenarios. The various risks associated with future climate change are subject to vulnerability, hazard, and exposure. Risks can be reduced by controlling exposure and vulnerability through adaptation

363 measures. To assess the impacts and examine the effects of adaptation, it is important to properly
364 represent the hazard due to climate change, and BC plays an important role in this regard. Bias-
365 corrected climate scenarios are expected to be useful for not only assessing heat risk but also for
366 various region-specific risk assessments.

## 367 7 Conclusions

368 We developed a new bias-corrected climate scenario using the multiple GCMs in CMIP6
369 and examined their applicability as inputs to impact studies. A comparison of the CMIP5-based
370 and CMIP6-based climate scenarios revealed that CMIP6-based scenarios had smaller biases in
371 temperature and precipitation for the underlying GCMs and the uncertainty in temperature in the
372 near future was relatively low, while there was a similar increasing trend for temperature and
373 precipitation under RCP2.6 and RCP8.5. Using the additional emissions scenario of RCP4.5 for
374 the CMIP6-based climate scenario would enable us to consider a wider range of possible futures.
375 The CDFDM-M successfully removed the inherent bias when the monthly values projected at
376 stations was compared to the observations.

377 To evaluate the climate scenarios, we analysed the representation of the heat mortality-
378 related indices and their dependency on the GWLs. The indices derived from the climate
379 scenarios showed good agreement with observations. The responses of TX35, TN25, and TN0 to
380 the GWLs were nonlinear. The MTX35 significantly increased when the GWL exceeded 2°C.
381 This indicated that the probability of MTX35 exceeding the 2018 case was 9.7% with a GWL of
382 1°C, but it would be 39.8% with a GWL of 2°C. The MTN25 increased with respect to global
383 warming even under a low GWL. If the GWL increased from 1°C to 2°C, the probability of
384 MTN25 exceeding 2018 was 2.7 times higher. The decrease in MTN0 was the most sensitive to
385 the GWL among the three indices analysed in this study. The probability of temperature falling
386 below MTN0 in the winter season of 2015/2016, when water shortage was a serious concern due
387 to a lack of snow accumulation, increased by 1.9 times when the GWL changed from 1°C to
388 2°C. These results indicate the need to accelerate the implementation of adaptation measures to
389 coming climate change. The IPCC reports (2018; 2021) have concluded that limiting global
390 warming to below 2°C is critical to minimize the impacts in many sectors in terms of the
391 adaptation strategies required for global warming, and our results support this. In addition, larger
392 uncertainty was found in the projection of MTX35 than in previous studies. Although we did not
393 consider the full range of GCM uncertainty, the results indicate that it is important to consider
394 the uncertainty due to the GCM used.

395 The application of climate scenarios to heat mortality-related indices showed that they
396 reproduced historical values well and would be useful for future projections. Our dataset is
397 expected to be utilized in various sectors to assess climate change impacts and to consider
398 adaptation strategies.

## 399 Acknowledgments

400 The authors are grateful to the anonymous reviewers for their constructive comments. This
401 research was supported by JST Grant NumberJPMJPF2013 and the Climate Change Adaptation
402 Research Program of NIES.
403

## Data availability

The downscaled data are publicly available at https://www.nies.go.jp/doi/10.17595/20210501.001-e.html in the NetCDF format. This dataset is bias corrected climate scenarios over Japan with the spatial resolution 1km using CMIP6. Five GCMs were selected from CMIP6; MIROC6, MRI-ESM2-0, ACCESS-CM2, IPSL-CM6A-LR, MPI-ESM1-2-HR. Daily data for eight variables (daily mean, max, min temperature, precipitation, solar radiation, downward longwave radiation, wind speed, and relative humidity) are avairable from 1900 to 2100 (1900-2014 is for historical and 2015-2100 is for future period). Regarding the GHGs emission pathways, SSP1-RCP2.6, SSP2-RCP4.5, and SSP5-RCP8.5 were used.

## References

Dosio, A.: Projections of climate change indices of temperature and precipitation from an ensemble of bias-adjusted high-resolution EURO-CORDEX regional climate models. J. Geophys. Res. Atmos., 121, 5488-5511, doi:10.1002/2015JD024411, 2016.

Fischer, E., Knutti, R.: Anthropogenic contribution to global occurrence of heavy-precipitation and high-temperature extremes. Nature Clim Change 5, 560–564. https://doi.org/10.1038/nclimate2617, 2015.

Fujibe F., Matsumoto, J., and Suzuki, H.: Regional Features of the Relationship between Daily Heat-Stroke Mortality and Temperature in Different Climate Zones in Japan, SOLA, 14, 144-147. doi:10.2151/sola.2018-025, 2018.

Gomez-Garcia, M., Matsumura, A., Ogawada, D., and Takahashi, K.: Time scale decomposition of climate and correction of variability using synthetic samples of stable distributions. Water Resources Research, 55, 3632-3658, https://doi.org/10.1029/2018WR023053, 2019.

Hanasaki, N., Takahashi, K., and Hijioka, Y.: Climate and socioeconomic scenarios for climate change impact and adaptation assessments in Japan. Environ. Sci., 25, 223−236, 2012 (in Japanese).

Hempel, S., Frieler, K., Warszawski, L., Schewe, J., and Piontek, F.: A trend-preserving bias correction – the ISI-MIP approach, Earth Syst. Dynam., 4, 219–236, https://doi.org/10.5194/esd-4-219-2013, 2013.

Iizumi, T., Nishimori, M., Ishigooka, Y., and Yokozawa, M.: Introduction to climate change scenario derived by statistical downscaling. J. Agri. Meteor., 66, 131−143, 2010 (in Japanese).

Iizumi, T., Nishimori, M., Dairaku, K., Adachi, S. A., and Yokozawa, M.: Evaluation and intercomparison of downscaled daily precipitation indices over Japan in present-day climate: Strengths and weaknesses of dynamical and biascorrection-type statistical downscaling methods. J. Geophys. Res. Atmos., 116, D01111, doi:10.1029/2010JD014513, 2011.

Iizumi, T., Takayabu, I., Dairaku, K., Kusaka, H., Nishimori, M., Sakurai, G., Ishizaki, N. N., Adachi, S. A., and Semenov, M. A.: Future change of daily precipitation indices in Japan: A stochastic weather generator-based bootstrap approach to provide probabilistic climate information. J. Geophys. Res. Atmos., 117, D11114, doi:10.1029/2011JD017197, 2012.

Iizumi, T., Okada, M. and Yokozawa, M.: A meteorological forcing data set for global crop modeling: Development, evaluation, and intercomparison. J. Geophys. Res. Atmos., 119, 363−384, doi:10.1002/2013JD020130, 2014.

Iizumi, T., Takikawa, H., Hirabayashi, Y., Hanasaki, N., and Nishimori, M.: Contribution of different bias-correction method and reference meteorological forcing data sets to uncertainty in projected temperature and precipitation extremes. J. Geophys. Res. Atmos., 122, 7800−7819, doi:10.1002/2017JD026613, 2017.

Imada, Y., Watanabe, M., Kawase, H., Shiogama, H., and Arai M.: The July 2018 high temperature event in Japan could not have happened without human-induced global warming. SOLA, 15A, 8-12, doi:10.2151/sola.15A-002, 2019.

IPCC: IPCC Special Report on the impacts of global warming of 1.5°C above pre-industrial levels and related global greenhouse gas emission pathways, in the context of strengthening the global response to the threat of climate change, sustainable development, and efforts to eradicate poverty. https://www.ipcc.ch/sr15/, 2018.

IPCC: Climate Change 2021: The Physical Science Basis. Contribution of Working Group I to the Sixth Assessment Report of the Intergovernmental Panel on Climate Change [Masson-Delmotte, V., Zhai, P., Pirani, A., Connors, S.L., Péan, C., Berger, S., Caud, N., Chen, Y., Goldfarb, L., Gomis, M. I., Huang, M., Leitzell, K., Lonnoy, E., Matthews, J.B.R., Maycock, T.K., Waterfield, T., Yelekçi, O., Yu, R., and Zhou, B. (eds.)]. Cambridge University Press. In Press, 2021.

Ishizaki, N. N., Nishimori, M., Iizumi, T., Shiogama, H., Hanasaki, N., and Takahashi K.: Evaluation of two bias-correction methods for gridded climate scenarios over Japan. SOLA, 16, 80-85, doi:10.2151/sola.2020-014, 2020.

Ishizaki, N. N.: Bias corrected climate scenarios over Japan based on CDFDM method using CMIP5, Ver.202005, NIES, doi:10.17595/20200415.001, 2020 (Reference date: 2022/1/11)

Ishizaki, N. N.: Bias corrected climate scenarios over Japan based on CDFDM method using CMIP6, Ver.1, NIES, doi:10.17595/20210501.001, 2021, (Reference date: 2022/1/11)

Iturbide, M., Casanueva, A., Bedia, J., Herrera, S., Milovac, J., and Gutiérrez, J. M.: On the need of bias adjustment for more plausible climate change projections of extreme heat. Atmospheric Science Letters, 23(2), e1072. https://doi.org/10.1002/asl.1072, 2022.

JMA and MEXT: Climate change in Japan 2020 ―Report on assessment of observed/projected climate change relating to the atmosphere, land and oceans. 272pp, 2020.

Kodera, S., Nishimura, T., Rashed, E. A., Hasegawa, K., Takeuchi, I., Egawa, R. and Hirata, A.: Estimation of heat-related morbidity from weather data: A computational study in three prefectures of Japan over 2013–2018. Environ. Int., 130, 104907, doi:10.1016/j.envint.2019.104907, 2019.

Maraun, D., Shepherd, T. G., Widmann, M., Zappa, G., Walton, D., Gutiérrez, J. M., Hagemann, S., Richter, I., Soares, P. M. M., Hall, A. and Mearns, L. O.: Towards process-informed bias correction of climate change simulations. Nature Clim Change 7, 764–773. https://doi.org/10.1038/nclimate3418, 2017.

MLIT: Regarding the drought of 2016. (Available online at: https://www.mlit.go.jp/common/001182356.pdf, accessed 21 Feb 2022), 2016.

Murata, A., Sasaki, H., Kawase, H., and Noasaka, M.: Evaluation of precipitation over an oceanic region of Japan in convection-permitting regional climate model simulations. Clim Dyn 48, 1779–1792. https://doi.org/10.1007/s00382-016-3172-x, 2017.

Ng, C. F. S., Ueda, K., Ono, M., Nitta, H., and Takami, A.: Characterizing the effect of summer temperature on heatstroke-related emergency ambulance dispatches in the Kanto area of Japan. Int J Biometeorol 58, 941–948. https://doi.org/10.1007/s00484-013-0677-4, 2014.

Ng, C. F. S., Boeckmann, M., Ueda, K., Zeeb, H., Nitta, H., Watanabe, C., and Honda, Y.: Heat-related mortality: Effect modification and adaptation in Japan from 1972 to 2010. Global Environmental Change, 39, 234-243. https://doi.org/10.1016/j.gloenvcha.2016.05.006, 2016.

Nishimori, M., Ishigooka, Y., Kuwagata, T., Takimoto, T. and Endo, N.: SI-CAT 1km-grid square regional climate projection scenario dataset for agricultural use (NARO2017). Journal of the Japan Society for Simulation Technology, 38, 150−154, 2019 (in Japanese).

Ohno, H., Sasaki, K., Ohara, G., and Nakazono, K.: Development of grid square air temperature and precipitation data compiled from observed, forecasted, and climatic normal data. Climate in Biosphere, 16, 71−79, 2016 (in Japanese).

Sasaki, H., Murata, A., Hanafusa, M., Oh'izumi, M., and Kurihara, K.: Reproducibility of present climate in a non-hydrostatic regional climate model nested within an atmosphere general circulation model. SOLA, 7, 173-176. https://doi.org/10.2151/sola.2011-044, 2011.

Shiogama H., Ishizaki, N. N., Hanasaki, N., Takahashi, K., Emori, S., Ito, R., Nakaegawa, T., Takayabu, I., Hijioka, Y., Takayabu, Y. N., and Shibuya, R.: Selecting CMIP6-Based Future Climate Scenarios for Impact and Adaptation Studies. SOLA, 17, 57-62, doi:10.2151/sola.2021-009, 2021.